

ODONATAN WING AND BODY MORPHOLOGIES

J.M. WAKELING¹

Department of Zoology, University of Cambridge, Downing Street,
Cambridge, CB2 3EJ, United Kingdom

Received January 12, 1996 / Revised and Accepted June 18, 1996

Parameters for shape, mass and virtual mass are described for the wings and bodies of 7 spp. The distribution of wing area and virtual mass follow precise allometric relationships, and these parameters can be predicted from the position of the centroid of area for each wing. Wing mass distributions show less clear trends due to specific effects of the pterostigmas. The different wing shapes between Anisoptera and Zygoptera are related to differences in their flight behaviours. No difference in wing shape was found between 'flier' and 'percher' groups of dragonfly. A clear relationship exists between the radii of the centre of mass and the second radius of gyration for the odon. bodies. The position of the centre of mass relative to the wing bases is related to the flight style and manoeuvrability of these insects.

INTRODUCTION

The design of dragonfly wings is the result of many compromises between the structural and aerodynamic demands required by each species. The extant Odonata consist of three suborders: Anisoptera, Anisozygoptera, and Zygoptera, which as their names suggest can be categorised by their relative wing shapes. Anisoptera are typified by large, strong and fast fliers able to turn rapidly on the spot; their fore- and hindwings are broad and of different shapes. In contrast, Zygoptera are characteristically smaller and fly slowly in any direction without turning their body (BRODSKY, 1994). They have almost identical fore- and hindwings which narrow towards their bases. The extant Anisozygoptera are a minor suborder with only two extant species and they have almost identical fore- and hindwings similar to the Zygoptera, but a body shape and anal appendages similar to the Anisoptera (RÜPPELL & HILFERT, 1993); these dragonflies are not considered further here.

¹ **Current address:** Gatty Marine Laboratory, University of St Andrews, East Sands, St Andrews, Fife, KY16 8LB, United Kingdom

This study addresses whether differences in the general flight behaviour of Anisoptera and Zygoptera can be correlated with wing morphology.

Various aspects of the functional relevance of wing features have been studied for Odonata. HERTEL (1966) described the wing of *Aeshna cyanea* as having a pleated structure near the leading edge, with strong veins top and bottom joined by thin membranes. These corrugations are deepest near the wing base and become shallower towards the tip and posterior wing margin; the combination of longitudinal veins and the membrane between them form a structure that is strong, light and resistant under normal conditions to transverse bending, although it is capable of local deformations to absorb sudden impacts at the wing tip (NEWMAN, 1982; NEWMAN & WOOTTON, 1986; WOOTTON, 1991). Corrugations give insect wings strength with scarcely any weight penalty (REES, 1975a), and the aerodynamic lift produced by these wings is no worse than that from airfoils with a smooth profile (REES, 1975b). Dragonfly wings have a serrated leading edge costa (HERTEL, 1966) which promotes the transition from laminar to turbulent flow over the wing, resulting in an increase in lift generated by the wing (NEWMAN et al., 1977). Small spurs have been noted on the surface of odonatan wings (HERTEL, 1966; NEWMAN et al., 1977; D'ANDREA & CARFI, 1988, 1989). Newman and co-workers showed that the height of these spurs was less than that for admissible roughness: "the amount of roughness which is considered 'admissible' in engineering applications is that maximum height of individual roughness elements which causes no increase in drag compared with a smooth wall" (SCHLICHTLING, 1968). Hence it is unlikely that these spurs have any aerodynamic function, a conclusion that has been misquoted by D'ANDREA & CARFI (1988, 1989). NEWMAN (1982) concluded that differences in the construction of the wings probably reflect the ways in which they are used in flight rather than their efficiency at performing their basic structural functions.

The wings flip over between the up- and downstrokes, and the supinated wing is effectively upside-down during the upstroke. Nonetheless, the wing camber also reverses so that it is in the correct sense for lift generation on each half stroke. ENNOS (1988) has shown that for Diptera the wing veins diverge posterodistally from a twistable leading edge, and aerodynamic loading on such a structure causes the wing to twist into camber of the correct sense. Odonatan wing veins conform to this model (MAGNAN, 1934; WOOTTON, 1991), and so camber generation may also be caused by the aerodynamic loading of the wing.

The pterostigma on dragonfly wings is a pigmented spot close to the leading edge near the wing tip. The pterostigma changes the mass distribution of the wing significantly, and effectively moves the centre of mass forward towards the torsion axis of the wing (NORBERG, 1972). This reduces inertial wing oscillations and flutter, thus raising the critical flight speed above which gliding becomes impossible. Nonetheless, the centre of mass is still behind the torsion axis for the wing, and wing twist at supination is probably caused by inertial forces acting on the wing

(NEWMAN, 1982).

A number of studies have measured first order mass and shape parameters that describe dragonflies, such as wing mass, wing area, distribution of wing area, wing loading, and moment of wing inertia. Allometries of these parameters have been compared to scaling with geometric similarity; departures from geometric similarity with changing size can suggest functional reasons for, or consequences of, trends in body and wing shape. Caution should be used when comparing the allometry of parameters with respect to body mass, as mean masses for a species can differ between seasons (MARDEN, 1989; GRABOW & RÜPPELL, 1995).

MAY (1981) found a relative increase in wing length with increasing body mass for Anisoptera, whereas NEWMAN (1982) and GRABOW & RÜPPELL (1995) report the opposite for Odonata in general. Whatever the precise scaling of wing length, all three of these studies show that there is good agreement between wing area and geometric scaling; thus larger dragonflies have higher wing loadings (body weight / wing area); the wing loading is a measure of how much lift a wing must generate per unit area. Presuming that the maximum lift coefficients are similar for wings of different dragonflies (WAKELING & ELLINGTON, 1997a), then the larger dragonflies must move their wings at higher velocities to generate the required lift. Indeed, flight speed is expected to be proportional to the square root of the wing loading (NORBERG & RAYNER, 1987). Field data for dragonfly flight speeds show a general increase with body size and thus wing loading (MAGNAN, 1934; NEVILLE, 1960; RÜPPELL, 1989), and the same is true for butterflies (BETTS & WOOTTON, 1988; CHAI & SRYGLEY, 1990; DUDLEY, 1990). It should be noted that maximum flight speed is additionally governed by factors such as maximum muscle power outputs and so is not directly related to wing loading. Damselflies do not show a systematic increase in wing loading with body mass because the heavier Calopterygidae have a disproportionately large wing area. However, the general wing loadings in damselflies are very much lower than those in dragonflies (GRABOW & RÜPPELL, 1995).

There are systematic differences between the shape and mass distributions of anisopteran and zygopteran wings. Among the Zygoptera (apart from the Calopterygidae), the outer half (by length) of the wing accounts for typically 67% of the wing-area; the corresponding figures are 60% for Calopterygidae, and 53% and 45% for Anisoptera fore- and hindwings, respectively (GRABOW & RÜPPELL, 1995). Various reasons have been put forward for the shape differences between dragonfly and damselfly wings based on flight velocity and wing inertia arguments (WOOTTON, 1991). The flapping speed of any chordwise element of the wing increases almost linearly from the wing base to the wing tip. For slow flight and hovering the wing base has very low velocity, and so there is a large ratio between the velocities of the wing tip and base; at fast speeds, on the other hand, the wing bases already have the forward velocity of the dragonfly, and so there is a lower ratio between the wing tip and base speeds. The lift produced by each seg-

ment of the wings is proportional to the square of the velocity of that segment. During slow flight, typical of the Zygoptera, the wing base cannot generate much lift because of its low velocity, and so the wing area is concentrated towards the wing tip where the velocities are greater. For the fast forward flight of Anisoptera the proximal wing region can generate useful lift and so has a larger proportion of the wing area; the inertial costs of accelerating the wing during each halfstroke are also minimised by concentrating the area, and thus mass, towards the wing base. However, the inertial power of both dragonflies and damselflies can be totally recovered regardless of assumptions about the degree of elastic energy storage in the thorax (WAKELING & ELLINGTON, 1997c), and so inertial arguments may not be appropriate for extant dragonfly species. Nonetheless, a modern dragonfly flying with petiolate, zygopteran-like wings would incur larger inertial costs that may significantly affect the power requirements for flight.

Aspect ratio is the ratio of twice the wing length to the mean wing chord, and the broad, low aspect ratio, dragonfly wings can be explained by their gliding flight (WOOTTON, 1991). Minimising drag during gliding is a compromise between minimising profile drag and induced drag from the wings (ENNOS, 1989). At the Reynolds numbers at which insects fly, profile drag increases with aspect ratio whereas induced drag decreases, and thus there is a particular aspect ratio for which drag can be minimised. ENNOS (1989) predicts that for gliding insects of 100 mg to 1 g the optimal aspect ratio should be between 5.0 and 7.9, respectively. Ennos uses ELLINGTON's (1984b) formula for predicting profile drag, but this is derived for hovering with large angles of incidence and overestimates the drag on gliding dragonfly wings (WAKELING & ELLINGTON, 1997a). Additionally, the induced drag from a pair of tandem wings is less than for isolated pairs of wings (PRANDTL & TIETJENS, 1957), and so the optimal aspect ratios for minimising drag during gliding will be greater than those predicted by ENNOS (1989).

ELLINGTON (1984a) describes how the use of the moments of area, virtual mass and wing mass and their non-dimensional radii can further the understanding of the aerodynamic properties of different wing morphologies. For example, the second moment of wing mass is equal to the moment of inertia for the wing, while in a quasi-steady analysis mean lift and profile power on the wings are proportional to the second and third moments of wing area respectively (WEIS-FOGH, 1973). Ellington's parameters have superseded the 'shape factors' used by WEIS-FOGH (1973) because the similar sets for describing wing mass and virtual mass are also useful for describing wing aerodynamics. There is currently a complete dearth of data on these morphological parameters for Odonata, and this study starts to redress this lack of information.

Moments of mass can be measured for the body in a similar way to the wings. Many insects beat their wings in a stroke plane that has a fixed inclination from their body axis, and a high degree of manoeuvrability is obtained with the centre of mass near the wing base and with a low moment of inertia, because the body will

respond quickly to desired changes in speed and direction (ELLINGTON, 1984a). Indeed, SRYGLEY & DUDLEY (1993) have shown that correlations do exist between manoeuvrability and the proximity of the centre of mass to the wing bases for a range of butterfly species. Zygoptera can vary their stroke plane angles with respect to their body axis (PFAU, 1986, WAKELING & ELLINGTON, 1997b), and so their turning speed is not limited by the body inertia.

Dragonflies can be categorised into two groups, 'fliers' and 'perchers' depending on their predominant flight behaviour (CORBET, 1983). Perchers observe their territories from their perch, whereas fliers do so on the wing. NEWMAN (1982) noted that fliers typically have longer abdomens than perchers, which increase the moments of body mass and thus damp down any turning moments generated by the wings; this may be a compromise between reducing manoeuvrability but increasing body stability during hovering, so the eyes are more effective at detecting prey. MAGNAN (1934) reports that the centre of mass lies between the fore- and hindwings in the flier *Anax parthenope*; however, he implicitly states that the non-dimensional hindwing base position is 0.35 body lengths posterior to the front. Measurements from scale drawings (ASKEW, 1988) suggest that for *A. parthenope* this non-dimensional hindwing base location is only 0.24, and for the 17 species of European Aeshnidae the mean position is 0.23, with the hindwing bases never being more than 0.28 body lengths from the front. Magnan's non-dimensional location for the centre of mass, occurring at 0.29 body lengths from the front was almost certainly behind both wing bases and would thus agree with Newman's observations for fliers.

Dragonflies can have among the highest flight muscle mass with respect to body mass of any insect (MARDEN, 1989), but the values are less for fliers than for perchers (MAY, 1981; MARDEN, 1987). In this study the first and second moments and radii of body mass are measured, as well as the thoracic muscle mass, for a range of dragonfly species, in order to help understand dragonfly body morphologies.

MATERIAL AND METHODS

The anisopteran species *Aeshna cyanea*, *Libellula depressa*, *L. quadrimaculata*, *Orthetrum cancellatum*, *Sympetrum sanguineum* and *S. striolatum*, and the zygopteran *Calopteryx splendens* were collected at Granchester Meadows, Milton Country Park, Quy Fen, and Wicken Fen in Cambridgeshire between May and August 1993. They were initially stored in dark specimen boxes, cooled with ice to about 4°C; all individuals were analysed for their morphology within 24 hours of capture.

During analysis the dragonflies were anaesthetised with CO₂ to aid handling them, and the mass m of the whole insect was measured on a Sartorius Research R200D balance to the nearest 0.01 mg. They were later killed by placing in a freezer for at least one hour.

Relationships were tested for similarity at the 5% significance level.

WING MASS PARAMETERS. – The left wings of each dragonfly were cut off at their bases and separately weighed for their mass m_w to the nearest 0.01 mg. They were then placed on a glass slide on a square grid with the long wing axis aligned along one of the sides of the grid. Strips 2-3 mm wide

were cut across the wing, starting from the wing base, resulting in n strips (typically 9-12) being cut for each wing. Immediately after each strip was cut it was weighed to the nearest 0.01 mg; each strip had mass m_i , and the distance r_i from the wing base to the centre of mass for each strip was taken as that to the centre of each strip.

Non-dimensional wing mass \hat{m}_w equals m_w/m , and the non-dimensional radial distance \hat{r} equals r/R , where R is the wing length. The following parameters were calculated from the distribution of mass within the wing according to ELLINGTON (1984a):

$$\text{kth moment of wing mass} \quad m_k = 2 \sum_{i=1}^n m_i r_i^k, \quad (1)$$

$$\text{Non-dimensional radius of kth moment of wing mass} \quad \hat{r}_k(m) = \left(\frac{m_k}{m_w R^k} \right)^{\frac{1}{k}}. \quad (2)$$

A small mass loss occurred each time a strip was cut resulting in $\sum m_i$ being typically 8% less than the initial mass. The k th moment of wing mass was corrected for this mass loss by multiplying it by the ratio of initial wing mass to $\sum m_i$ in accordance with ELLINGTON (1984a).

WING SHAPE PARAMETERS. – The right wings of each dragonfly were cut off at their bases; they were each weighed for their mass m_w to the nearest 0.01 mg, and maximum length R was measured with Vernier calipers to the nearest 0.01 mm. The wings were then photocopied at $\times 2$ enlargement, and this image was taken into a Macintosh IIcx computer via a Panasonic BL600 video camera coupled to a Neotech ImageGrabber24 card. A grid of 51 equally spaced parallel lines was superimposed onto the wing image, with the lines perpendicular to the major wing axis. The points of intersection of this grid and the wing outline were digitised and represent the corners of 50 adjacent parallelograms within the wing shape. Each parallelogram has area s_i and mean length c_i (the mean wing chord for the strip). Due to pixellation errors from the image grabber board, square objects were grabbed with one side 0.3% longer than the other; this error was less than that for the other procedures in morphology analysis, and so was ignored.

The following parameters were calculated from the distribution of wing area according to ELLINGTON (1984a). g is equal to gravitational acceleration, ρ is air density (1.205 kg m^{-3}) and ρ_w is wing density (1200 kg m^{-3}):

$$\text{Wing area} \quad S = 2 \sum_{i=1}^{50} s_i, \quad (3)$$

$$\text{Aspect ratio} \quad AR = \frac{4R^2}{S}, \quad (4)$$

$$\text{Wing loading} \quad p_w = \frac{mg}{S}, \quad (5)$$

$$\text{Non-dimensional mean wing thickness} \quad \hat{h} = \frac{m_w}{\rho_w SR} \quad (6)$$

$$\text{kth moment of wing area} \quad S_k = 2 \sum_{i=1}^{50} s_i r_i^k, \quad (7)$$

$$\text{Non-dimensional radius of kth moment of area} \quad \hat{r}_k(S) = \left(\frac{S_k}{SR^k} \right)^{\frac{1}{k}}, \quad (8)$$

Virtual mass
$$v = \frac{\rho\pi}{2} \sum_{i=1}^{50} c_i s_i, \quad (9)$$

Non-dimensional virtual mass
$$\hat{v} = \frac{v(AR)^2}{2\rho\pi R^3}, \quad (10)$$

k th moment of virtual mass
$$v_k = \frac{\rho\pi}{2} \sum_{i=1}^{50} c_i s_i^k, \quad (11)$$

Non-dimensional radius of k th moment of virtual mass
$$\hat{r}_k(v) = \left(\frac{v_k}{vR^k} \right)^{\frac{1}{k}}. \quad (12)$$

BODY PARAMETERS. – The mass of the body without the wings, m_b , was weighed to the nearest 0.01 g, and its maximum length L to the tip of the genitalia measured with Vernier calipers to the nearest 0.01 mm. The bodies were then frozen for at least one hour to make them rigid; the freezing procedures produced no perceivable change in mass from m_b , and it was assumed that the position of the centre of mass also remained unaffected. Video images of the bodies adjacent to plumb lines were taken with the bodies suspended by a pin through the top of the first abdominal segment and then with a pin through the forewing bases. These images were later analysed by drawing lines through the pin positions, and parallel to the respective plumb lines. The lines intersect at the position of the centre of mass, which is at distances l from the tip of the head and l_1 from the forewing base axis. With the pin still through the forewing bases, the period of oscillation of the body swinging as a pendulum was measured. An infrared light beam was set up so that it was broken on each half cycle of the oscillation; a signal from the beam was displayed on an oscilloscope, and the period t for each oscillation thus measured.

Non-dimensional body length \hat{l} equals l/L . The moment of inertia of the body and second radius of gyration were calculated according to ELLINGTON (1984a):

Moment of inertia of body
$$I_b = \frac{l_1 m_b g t^2}{4\pi^2}, \quad (13)$$

Non-dimensional radius of gyration of I_b
$$\hat{l}_2 = \left(\frac{I_b}{m_b L^2} \right)^{\frac{1}{2}}. \quad (14)$$

The head, abdomen and legs were finally removed from the thorax with a scalpel, and the thorax was weighed to the nearest 0.01 mg. The thorax was submersed in boiled water for 30 seconds and allowed to float in the water for a further five minutes. The softened thorax was then bisected between the wing bases, and the muscles removed with a pair of forceps. What remained was mainly thoracic cuticle, and this was air dried on paper tissue for 24 hours before a final weighing. The thoracic muscle mass m_m was taken to be the difference in mass between the fresh thorax and that with the muscle removed. This will slightly over-estimate the muscle mass because it will include the mass of other tissue such as tracheae that was also removed, but the error should be small. Non-dimensional muscle mass $\hat{m}_m = m_m/m$.

RESULTS

Of the seven species studied, *Aeshna cyanea* is a flier and the rest are perchers. The reason for the imbalance partly reflects the ease at catching stationary perchers from their perch compared to catching fliers on the wing. The damselfly

Calopteryx splendens is a percher, as are all damselflies, but for the purposes of comparison it is treated separately from the anisopteran perchers *Libellula depressa*, *L. quadrimaculata*, *Orthetrum cancellatum*, *Sympetrum sanguineum* and *S. striolatum*. It should be noted that the Calopterygidae are atypical of damselflies in that they have a disproportionately high wing area (GRABOW & RÜPPELL, 1995).

WING PARAMETERS

The measured wing parameters are given in Table I for the forewings and Table II for the hindwings; Table I additionally gives the identification code, ID, and the body mass and wing loading for the odonates. The data for the non-dimensional radii are plotted in Figures 1-4. It is clear from Figure 1 that there are three classes of wing shape for these species. Anisopteran hindwings are broad-based, with their centroid of wing area within the proximal half of the wing. Anisopteran forewings have their wing area more evenly distributed, with the centroid of area just distal to the midpoint of the wing; they also show less variation in shape than the hindwings. Zygopteran fore- and hindwings are indistinguishable from each other in both shape and mass distribution, and the majority of their area is in the distal half of the wing.

The relations between the non-dimensional moments of wing area, mass and virtual mass have not been explained and have been coined 'laws of wing shape': rules that are obeyed even if the reasons for doing so are unknown (ELLINGTON,

Table I
Morphological wing parameters for Odonata forewings

| species | sex | ID | m | Pu | m _w | R | S | AR | r ₁ (S) | r ₂ (S) | r ₃ (S) | v | r ₁ (v) | r ₂ (v) | m _w (%) | h(%) | r ₁ (m) | r ₂ (m) |
|------------------------------|-------|-------|--------|-------------------|----------------|--------|-----------------|--------|--------------------|--------------------|--------------------|-------|--------------------|--------------------|--------------------|--------|--------------------|--------------------|
| | | | mg | N m ⁻¹ | mg | mm | mm ² | | | | | | | | | | | |
| <i>Archaeocyanea</i> | M | AC1 | 677.1 | 2.97 | 8.92 | 49.87 | 954.19 | 18.43 | 0.517 | 0.377 | 0.628 | 0.661 | 0.518 | 0.377 | 1.32 | 0.8153 | 0.133 | 0.443 |
| | F | AC2 | 1085.6 | 3.02 | 11.02 | 51.55 | 931.91 | 11.38 | 0.507 | 0.568 | 0.613 | 0.663 | 0.514 | 0.364 | 1.01 | 0.9192 | 0.148 | 0.479 |
| | F | AC3 | 1162.3 | 3.38 | 9.60 | 30.05 | 892.16 | 11.23 | 0.305 | 0.567 | 0.613 | 0.654 | 0.511 | 0.363 | 0.85 | 0.9185 | 0.316 | 0.415 |
| | F | AC4 | 818.2 | 3.76 | 9.08 | 31.95 | 1167.29 | 10.91 | 0.517 | 0.377 | 0.621 | 0.661 | 0.530 | 0.379 | 1.11 | 0.9130 | 0.391 | 0.484 |
| | F | AC5 | 664.7 | 2.71 | 6.85 | 32.20 | 1007.73 | 10.82 | 0.508 | 0.378 | 0.621 | 0.666 | 0.532 | 0.390 | 1.06 | 0.9188 | 0.365 | 0.451 |
| F | AC6 | 567.6 | 2.52 | 6.30 | 30.70 | 972.01 | 10.58 | 0.513 | 0.377 | 0.614 | 0.669 | 0.523 | 0.371 | 1.14 | 0.9109 | 0.383 | 0.464 | |
| <i>Libellula depressa</i> | M | LJ1 | 443.6 | 3.72 | 1.57 | 36.52 | 321.86 | 10.22 | 0.503 | 0.568 | 0.613 | 0.643 | 0.509 | 0.362 | 1.03 | 0.9188 | 0.321 | 0.481 |
| | M | LJ8 | 339.0 | 3.76 | | 34.47 | 462.46 | 10.28 | 0.518 | 0.379 | 0.622 | 0.658 | 0.531 | 0.381 | | | | |
| | M | LJ16 | 375.8 | 3.16 | 4.10 | 37.79 | 515.38 | 10.84 | 0.506 | 0.370 | 0.616 | 0.643 | 0.511 | 0.366 | 1.10 | 0.9177 | 0.359 | 0.490 |
| | M | LJ18 | 295.0 | 2.49 | 3.04 | 36.53 | 516.79 | 10.33 | 0.508 | 0.371 | 0.616 | 0.649 | 0.517 | 0.369 | 1.71 | 0.9218 | 0.345 | 0.482 |
| | M | LJ29 | 385.0 | 4.47 | 4.21 | 35.99 | | | | | | | | | | | 0.245 | 0.523 |
| M | LJ20 | 377.9 | 3.19 | 4.27 | 36.44 | 524.02 | 10.14 | 0.508 | 0.370 | 0.615 | 0.652 | 0.514 | 0.364 | 1.13 | 0.9184 | 0.370 | 0.497 | |
| M | LJ1 | 408.9 | 3.49 | 4.17 | 36.76 | 522.47 | 10.34 | 0.514 | 0.376 | 0.621 | 0.652 | 0.535 | 0.377 | 1.15 | 0.9204 | 0.371 | 0.484 | |
| <i>Orthetrum cancellatum</i> | M | OC1 | 415.8 | 3.17 | 4.30 | 38.47 | 567.73 | 10.42 | 0.498 | 0.563 | 0.609 | 0.640 | 0.499 | 0.355 | 1.08 | 0.9173 | 0.344 | 0.491 |
| | M | OC2 | 609.1 | 3.65 | 4.73 | 39.49 | | | | | | | | | 1.05 | | 0.341 | 0.481 |
| | M | OC3 | 443.7 | 3.75 | 4.97 | 39.43 | | | | | | | | | 1.12 | | 0.351 | 0.483 |
| | M | OC4 | 443.1 | 3.24 | 4.81 | 38.54 | 399.26 | 10.08 | 0.497 | 0.562 | 0.608 | 0.644 | 0.499 | 0.354 | 1.04 | 0.9169 | | |
| | M | OC5 | 415.0 | 3.86 | 4.79 | 39.97 | 618.02 | 10.34 | 0.499 | 0.563 | 0.610 | 0.644 | 0.500 | 0.355 | 1.04 | 0.9165 | 0.258 | 0.489 |
| | M | OC6 | 382.1 | 3.91 | 3.85 | 38.36 | 562.51 | 10.46 | 0.501 | 0.563 | 0.611 | 0.645 | 0.504 | 0.358 | 1.01 | 0.9147 | 0.346 | 0.486 |
| | M | OC7 | 330.7 | 2.57 | 3.91 | 40.06 | 396.87 | 10.75 | 0.501 | 0.564 | 0.610 | 0.650 | 0.503 | 0.356 | 1.11 | 0.9136 | 0.410 | 0.493 |
| <i>Sympetrum sanguineum</i> | M | SSa1 | 135.3 | 1.69 | 1.57 | 28.62 | 341.66 | 9.78 | 0.511 | 0.573 | 0.617 | 0.648 | 0.530 | 0.372 | 1.16 | 0.9226 | 0.449 | 0.535 |
| | M | SSa2 | 121.9 | 1.61 | 1.59 | 27.85 | 327.37 | 9.47 | 0.507 | 0.570 | 0.615 | 0.648 | 0.514 | 0.367 | 1.30 | 0.9226 | 0.450 | 0.538 |
| | M | SSa3 | 114.0 | 1.61 | 1.07 | 28.95 | 305.99 | 9.49 | 0.513 | 0.575 | 0.620 | 0.652 | 0.523 | 0.376 | 0.93 | 0.9206 | 0.466 | 0.488 |
| | M | SSa4 | 125.5 | 1.69 | 1.40 | 27.80 | 318.00 | 9.72 | 0.515 | 0.576 | 0.620 | 0.654 | 0.528 | 0.378 | 1.11 | 0.9234 | 0.463 | 0.548 |
| | M | SSa5 | 133.0 | 1.87 | 1.36 | 27.23 | 312.38 | 9.49 | 0.513 | 0.574 | 0.618 | 0.660 | 0.524 | 0.374 | 1.17 | 0.9241 | 0.481 | 0.565 |
| | M | SSa6 | 111.5 | 1.63 | 1.22 | 26.38 | 297.39 | 9.51 | 0.507 | 0.570 | 0.616 | 0.647 | 0.515 | 0.368 | 1.09 | 0.9188 | 0.453 | 0.517 |
| | M | SSa7 | 138.5 | 1.76 | 1.50 | 28.78 | 321.89 | 9.41 | 0.514 | 0.575 | 0.619 | 0.657 | 0.525 | 0.376 | 1.01 | 0.9219 | 0.437 | 0.516 |
| | M | SSa8 | 108.4 | 1.59 | 1.24 | 26.16 | 296.18 | 9.24 | 0.518 | 0.577 | 0.621 | 0.655 | 0.530 | 0.379 | 1.14 | 0.9234 | 0.466 | 0.551 |
| | M | SSa9 | 139.3 | 1.67 | 1.60 | 29.44 | 327.44 | 9.78 | 0.507 | 0.578 | 0.614 | 0.650 | 0.515 | 0.368 | 1.14 | 0.9224 | 0.439 | 0.511 |
| M | SSa10 | 132.6 | 1.76 | 1.56 | 26.14 | 326.77 | 9.42 | 0.508 | 0.567 | 0.613 | 0.648 | 0.510 | 0.363 | 1.26 | 0.9229 | 0.424 | 0.503 | |
| <i>Sympetrum striolatum</i> | M | SSt1 | 155.9 | 1.75 | 2.63 | 31.84 | 396.82 | 10.22 | 0.507 | 0.578 | 0.615 | 0.648 | 0.514 | 0.367 | 1.71 | 0.9182 | 0.452 | 0.518 |
| | F | SSt2 | 122.9 | 1.73 | 2.03 | 31.22 | 405.82 | 9.63 | 0.399 | 0.570 | 0.614 | 0.648 | 0.511 | 0.369 | 1.65 | 0.9111 | 0.449 | 0.524 |
| | F | SSt3 | 123.6 | 1.75 | 2.05 | 31.77 | 416.82 | 9.69 | 0.513 | 0.574 | 0.618 | 0.659 | 0.524 | 0.374 | 1.81 | 0.9209 | 0.451 | 0.544 |
| | M | SSt4 | 108.0 | 1.27 | 1.82 | 30.65 | 378.49 | 9.54 | 0.515 | 0.568 | 0.613 | 0.649 | 0.511 | 0.364 | 1.66 | 0.9221 | 0.408 | 0.501 |
| | F | SSt5 | 118.9 | 1.30 | 2.08 | 31.14 | 394.88 | 9.76 | 0.512 | 0.574 | 0.618 | 0.655 | 0.523 | 0.374 | 1.75 | 0.9177 | 0.388 | 0.477 |
| | M | SSt6 | 125.9 | 1.76 | 2.06 | 29.95 | 381.81 | 9.39 | 0.503 | 0.568 | 0.613 | 0.653 | 0.509 | 0.363 | 1.62 | 0.9199 | 0.399 | 0.486 |
| | M | SSt7 | 109.1 | 1.27 | 1.69 | 30.13 | 379.52 | 9.36 | 0.506 | 0.569 | 0.614 | 0.644 | 0.512 | 0.365 | 1.36 | 0.9219 | 0.416 | 0.500 |
| | M | SSt8 | 131.7 | 1.49 | 1.91 | 30.84 | 385.76 | 9.86 | 0.508 | 0.572 | 0.617 | 0.645 | 0.517 | 0.371 | 1.45 | 0.9224 | 0.418 | 0.521 |
| | M | SSt9 | | | | 1.74 | 21.36 | | | | | | | | | | 0.453 | 0.531 |
| | M | SSt10 | | | | 1.81 | 20.43 | 454.73 | 8.52 | 0.518 | 0.601 | 0.639 | 1.113 | 0.574 | 0.613 | 2.03 | 0.9115 | 0.424 |
| <i>Calopteryx splendens</i> | M | CS1 | 91.0 | 1.06 | | 29.44 | 400.31 | 8.66 | 0.533 | 0.604 | 0.641 | 1.126 | 0.580 | 0.617 | 1.71 | 0.9115 | 0.424 | 0.487 |
| | M | CS2 | 123.6 | 1.45 | 1.60 | 30.42 | 427.32 | 8.66 | 0.532 | 0.603 | 0.641 | 1.132 | 0.578 | 0.616 | 1.54 | 0.9120 | 0.446 | 0.478 |
| | M | CS3 | 119.1 | 1.20 | | 29.66 | 398.25 | 8.82 | 0.537 | 0.607 | 0.644 | 1.132 | 0.587 | 0.623 | 1.36 | 0.9117 | 0.440 | 0.510 |
| | M | CS4 | 119.1 | 1.20 | | 29.66 | 398.25 | 8.82 | 0.537 | 0.607 | 0.644 | 1.132 | 0.587 | 0.623 | 1.36 | 0.9117 | 0.440 | 0.510 |
| | M | CS5 | 105.6 | 1.25 | 1.92 | 30.44 | 424.80 | 8.72 | 0.543 | 0.598 | 0.637 | 1.109 | 0.569 | 0.609 | 1.81 | 0.9122 | 0.417 | 0.491 |
| | M | CS6 | 88.2 | 1.00 | 1.70 | 29.16 | 411.13 | 8.83 | 0.536 | 0.606 | 0.644 | 1.125 | 0.585 | 0.622 | 1.62 | 0.9119 | 0.453 | 0.526 |
| | M | CS7 | 81.8 | 1.12 | 1.31 | 27.11 | 375.79 | 8.17 | 0.547 | 0.600 | 0.639 | 1.109 | 0.576 | 0.615 | 1.60 | 0.9105 | 0.450 | 0.520 |

1984a). Allometric equations that describe the relationships between $\hat{r}_2(S)$ and $\hat{r}_3(S)$ with $\hat{r}_1(S)$, and $\hat{r}_2(v)$ with $\hat{r}_1(v)$ are given by:

$$\hat{r}_2(S) = 0.919\hat{r}_1(S)^{0.706}, \tag{15}$$

$$\hat{r}_3(S) = 0.886\hat{r}_1(S)^{0.541}, \tag{16}$$

$$\hat{r}_2(v) = 0.925\hat{r}_1(v)^{0.738}. \tag{17}$$

All these relationships are slightly but significantly different from those given by ELLINGTON (1984a) for a diverse range of 20 different insect species from six orders. It is no surprise that one particular order, Odonata in this case, has slightly different wing shape functions from insects in general. Nonetheless, within the Odonata there are universal laws of wing shape, given by equations (15) to (17), which can be used to predict higher non-dimensional radii from the first non-dimensional radius of area and virtual mass. The allometric equation to describe the

Table II
Morphological wing parameters for Odonata hindwings

| ID | m_w mg | R mm | S mm ² | AR | $\hat{r}_1(S)$ | $\hat{r}_2(S)$ | $\hat{r}_3(S)$ | \hat{v} | $\hat{r}_1(v)$ | $\hat{r}_2(v)$ | $m_w(\%)$ | $h(\%)$ | $\hat{r}_1(m)$ | $\hat{r}_2(m)$ |
|--------|-------------|---------|----------------------|-------|----------------|----------------|----------------|-----------|----------------|----------------|-----------|---------|----------------|----------------|
| AC1 | 10.04 | 48.65 | 1284.84 | 7.37 | 0.460 | 0.530 | 0.581 | 1.052 | 0.432 | 0.496 | 1.48 | 0.0113 | 0.327 | 0.450 |
| AC2 | 12.79 | 50.11 | 1186.77 | 8.46 | 0.464 | 0.530 | 0.579 | 1.074 | 0.439 | 0.497 | 1.18 | 0.0179 | 0.346 | 0.479 |
| AC3 | 11.44 | 48.44 | 1151.14 | 8.15 | 0.465 | 0.534 | 0.585 | 1.052 | 0.438 | 0.502 | 0.98 | 0.0172 | 0.324 | 0.425 |
| AC4 | 10.57 | 53.39 | 1067.29 | 10.68 | 0.466 | 0.533 | 0.583 | 1.065 | 0.440 | 0.500 | 1.29 | 0.0120 | 0.363 | 0.447 |
| AC5 | 8.03 | 52.08 | 1328.30 | 8.17 | 0.476 | 0.541 | 0.589 | 1.069 | 0.456 | 0.514 | 1.24 | 0.0099 | 0.370 | 0.453 |
| AC6 | 6.54 | 50.24 | 1238.79 | 8.15 | 0.468 | 0.535 | 0.584 | 1.066 | 0.443 | 0.503 | 1.15 | 0.0084 | 0.337 | 0.420 |
| LD1 | 4.71 | 35.11 | 649.48 | 7.99 | 0.448 | 0.521 | 0.573 | 1.053 | 0.412 | 0.481 | 1.06 | 0.0163 | 0.320 | 0.464 |
| LQ8 | | 33.44 | 598.38 | 7.48 | 0.457 | 0.527 | 0.578 | 1.059 | 0.425 | 0.490 | | | | |
| LQ16 | 4.92 | 36.14 | 645.08 | 8.10 | 0.446 | 0.521 | 0.574 | 1.056 | 0.406 | 0.478 | 1.31 | 0.0176 | 0.343 | 0.484 |
| LQ18 | 6.10 | 35.43 | 646.56 | 7.76 | 0.447 | 0.522 | 0.575 | 1.055 | 0.408 | 0.479 | 2.07 | 0.0214 | 0.327 | 0.438 |
| LQ29 | 5.03 | 34.66 | | | | | | | | | 1.31 | | 0.366 | 0.478 |
| LQ30 | 5.27 | 35.43 | 646.46 | 7.76 | 0.451 | 0.525 | 0.577 | 1.052 | 0.414 | 0.484 | 1.39 | 0.0190 | 0.333 | 0.454 |
| LQ31 | 5.82 | 35.28 | 626.28 | 7.95 | 0.465 | 0.532 | 0.581 | 1.075 | 0.437 | 0.497 | 1.42 | 0.0231 | 0.349 | 0.460 |
| OC1 | 5.53 | 37.17 | 735.91 | 7.51 | 0.441 | 0.515 | 0.568 | 1.061 | 0.402 | 0.470 | 1.33 | 0.0161 | 0.375 | 0.425 |
| OC2 | 5.51 | 37.85 | 779.10 | 7.36 | 0.437 | 0.512 | 0.565 | 1.064 | 0.394 | 0.464 | 1.23 | 0.0156 | 0.315 | 0.460 |
| OC3 | 5.89 | 37.96 | 757.35 | 7.61 | 0.443 | 0.516 | 0.569 | 1.061 | 0.404 | 0.472 | 1.33 | 0.0174 | 0.317 | 0.461 |
| OC4 | 5.40 | 37.08 | 753.81 | 7.30 | 0.442 | 0.515 | 0.568 | 1.063 | 0.402 | 0.470 | 1.22 | 0.0161 | 0.321 | 0.447 |
| OC5 | 5.96 | 39.56 | 806.95 | 7.76 | 0.440 | 0.514 | 0.568 | 1.061 | 0.399 | 0.469 | 1.43 | 0.0150 | 0.302 | 0.439 |
| OC6 | 4.99 | 37.37 | 724.95 | 7.71 | 0.442 | 0.517 | 0.570 | 1.056 | 0.402 | 0.472 | 1.31 | 0.0148 | 0.311 | 0.438 |
| OC7 | 4.34 | 38.47 | 740.51 | 7.99 | 0.449 | 0.521 | 0.573 | 1.059 | 0.415 | 0.481 | 1.24 | 0.0124 | 0.313 | 0.449 |
| SSan1 | 1.72 | 27.63 | 443.77 | 6.88 | 0.446 | 0.520 | 0.573 | 1.052 | 0.409 | 0.479 | 1.27 | 0.0118 | 0.432 | 0.526 |
| SSan2 | 1.70 | 26.90 | 413.45 | 7.00 | 0.446 | 0.520 | 0.573 | 1.052 | 0.407 | 0.478 | 1.39 | 0.0124 | 0.400 | 0.495 |
| SSan3 | 1.29 | 26.01 | 389.19 | 6.95 | 0.449 | 0.524 | 0.577 | 1.046 | 0.414 | 0.485 | 1.13 | 0.0103 | 0.414 | 0.507 |
| SSan4 | 1.83 | 27.04 | 410.77 | 7.12 | 0.451 | 0.522 | 0.574 | 1.058 | 0.417 | 0.484 | 1.45 | 0.0140 | 0.372 | 0.466 |
| SSan5 | 1.81 | 26.17 | 400.96 | 6.83 | 0.447 | 0.521 | 0.574 | 1.05 | 0.411 | 0.481 | 1.36 | 0.0129 | 0.385 | 0.490 |
| SSan6 | 1.60 | 25.49 | 380.01 | 6.84 | 0.453 | 0.525 | 0.577 | 1.05 | 0.422 | 0.489 | 1.43 | 0.0137 | 0.398 | 0.499 |
| SSan7 | 1.78 | 27.46 | 428.40 | 7.04 | 0.446 | 0.521 | 0.574 | 1.051 | 0.409 | 0.480 | 1.29 | 0.0126 | 0.412 | 0.499 |
| SSan8 | 1.31 | 24.94 | 372.37 | 6.68 | 0.450 | 0.525 | 0.576 | 1.048 | 0.417 | 0.486 | 1.20 | 0.0153 | 0.419 | 0.520 |
| SSan9 | 1.96 | 28.54 | 460.24 | 7.08 | 0.444 | 0.519 | 0.572 | 1.054 | 0.406 | 0.476 | 1.41 | 0.0123 | 0.384 | 0.481 |
| SSan10 | 1.72 | 26.70 | 404.00 | 7.06 | 0.447 | 0.521 | 0.573 | 1.053 | 0.412 | 0.481 | 1.28 | 0.0128 | 0.406 | 0.495 |
| SS1 | 2.72 | 29.72 | 465.45 | 7.59 | 0.446 | 0.521 | 0.575 | 1.049 | 0.407 | 0.479 | 1.76 | 0.0165 | 0.409 | 0.502 |
| SS2 | 2.34 | 30.37 | 505.87 | 7.29 | 0.449 | 0.521 | 0.573 | 1.057 | 0.416 | 0.482 | 1.90 | 0.0124 | 0.358 | 0.449 |
| SS3 | 2.38 | 30.90 | 542.23 | 7.04 | 0.456 | 0.527 | 0.578 | 1.059 | 0.425 | 0.490 | 2.11 | 0.0119 | 0.405 | 0.499 |
| SS4 | 2.25 | 28.80 | 457.58 | 7.25 | 0.449 | 0.524 | 0.577 | 1.047 | 0.412 | 0.485 | 2.08 | 0.0128 | 0.377 | 0.475 |
| SS5 | 2.16 | 29.73 | 500.44 | 7.06 | 0.452 | 0.525 | 0.577 | 1.051 | 0.419 | 0.487 | 1.82 | 0.0118 | 0.383 | 0.471 |
| SS6 | 2.48 | 29.70 | 488.01 | 7.23 | 0.447 | 0.522 | 0.575 | 1.049 | 0.410 | 0.481 | 1.97 | 0.0153 | 0.376 | 0.471 |
| SS7 | 2.00 | 28.97 | 465.20 | 7.21 | 0.442 | 0.518 | 0.571 | 1.053 | 0.403 | 0.473 | 1.83 | 0.0120 | 0.383 | 0.483 |
| SS8 | 2.35 | 29.59 | 480.08 | 7.30 | 0.450 | 0.525 | 0.578 | 1.045 | 0.414 | 0.487 | 1.78 | 0.0125 | 0.368 | 0.464 |
| SS9 | 2.11 | 29.68 | | | | | | | | | | | 0.400 | 0.484 |
| CS1 | 1.81 | 29.36 | 381.95 | 9.03 | 0.565 | 0.613 | 0.649 | 1.159 | 0.593 | 0.628 | 1.98 | 0.0135 | 0.416 | 0.490 |
| CS2 | 1.65 | 28.77 | 387.11 | 8.55 | 0.553 | 0.604 | 0.642 | 1.118 | 0.579 | 0.618 | 1.76 | 0.0124 | 0.441 | 0.508 |
| CS3 | 1.84 | 29.28 | 406.92 | 8.42 | 0.551 | 0.603 | 0.641 | 1.119 | 0.577 | 0.615 | 1.49 | 0.0112 | 0.444 | 0.511 |
| CS4 | 1.70 | 29.14 | 380.53 | 8.93 | 0.557 | 0.607 | 0.645 | 1.126 | 0.585 | 0.622 | 1.43 | 0.0125 | 0.425 | 0.500 |
| CS5 | 1.90 | 29.49 | 406.70 | 8.55 | 0.549 | 0.601 | 0.640 | 1.115 | 0.573 | 0.612 | 1.80 | 0.0133 | 0.439 | 0.505 |
| CS6 | 1.79 | 29.06 | 406.89 | 8.30 | 0.549 | 0.602 | 0.641 | 1.109 | 0.576 | 0.616 | 2.02 | 0.0123 | 0.423 | 0.491 |
| CS7 | 1.36 | 27.04 | 342.20 | 8.54 | 0.550 | 0.603 | 0.642 | 1.107 | 0.579 | 0.619 | 1.66 | 0.0121 | 0.420 | 0.487 |

relation between $\hat{r}_1(v)$ with $\hat{r}_1(S)$ is

$$\hat{r}_1(v) = 1.592\hat{r}_1(S)^{1.679}. \quad (18)$$

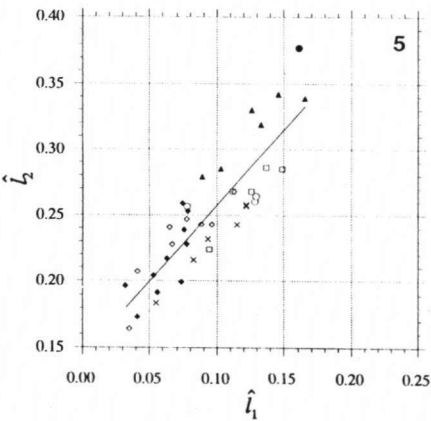
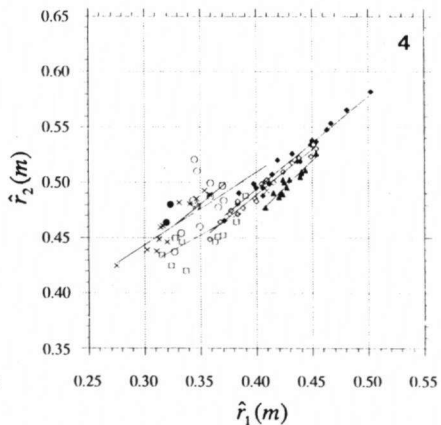
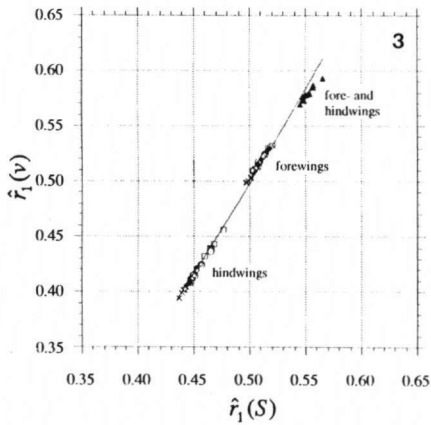
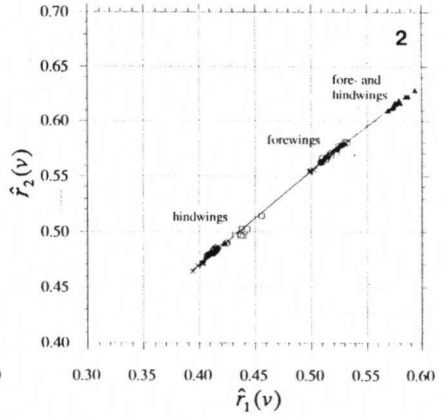
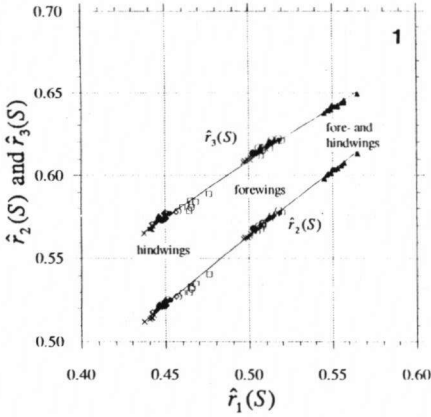
A combination of equations (15) to (18) can be used to predict the non-dimensional radii of area and virtual mass for these odonates from the centroid of area, $\hat{r}_1(S)$ with a mean error of 0.5% and never more than 2.9%; the relationships from ELLINGTON (1984a) would predict these radii with a mean error of 1.1% and never more than 2.7%. Both sets of estimations are within the intraspecific variation for these radii. Figure 3 shows that the allometric relationship between $\hat{r}_1(v)$ and $\hat{r}_1(S)$ does not fit the data for *C. splendens* as well as for the Anisoptera. The allometric relationships between $\hat{r}_1(v)$ and $\hat{r}_1(S)$ are significantly different for the anisoptera and *C. splendens*; the relationship for the Anisoptera is also significantly different from equation (18) and that in ELLINGTON (1984a), and is

$$\hat{r}_1(v) = 1.720\hat{r}_1(S)^{1.781}. \quad (19)$$

Predicting the non-dimensional radii of area and virtual mass for Anisoptera using equations (15) to (17) and equation (19) results in a mean error of 0.3% and never more than 1.4% error. A more detailed study is required if $\hat{r}_1(v)$ is to be predicted accurately from $\hat{r}_1(S)$ for Zygoptera. No allometric relationship is given between $\hat{r}_1(v)$ and $\hat{r}_1(S)$ for Zygoptera as the data available are only from one species, *C. splendens*.

The non-dimensional radii for wing mass are much more variable than those for area and virtual mass. $\hat{r}_2(m)$ shows a positive allometry with $\hat{r}_1(m)$, but there are different allometries for each species. The reason for this variability is largely due to the effect of the pterostigmas on the mass distribution. The pterostigma has been described as an inertial regulator of wing pitch by changing the centre of wing mass and the moment of inertia of the wing (NORBERG, 1972). Different pterostigmas occur for each species, and their effect on the non-dimensional moments of mass is thus also different for each species. There is no general allometric relationship that will predict $\hat{r}_2(m)$ from $\hat{r}_1(m)$ for Odonata.

Figs 1-5. The allometric relationships (indicated by the curves): (1) Radii of the second and third moments of wing area, $\hat{r}_2(S)$ and $\hat{r}_3(S)$, plotted against the position of the centroid $\hat{r}_1(S)$; - (2) Radius of the gyration of the virtual wing mass $\hat{r}_2(v)$, plotted against its centroid $\hat{r}_1(v)$; - (3) Positions of the centroids of virtual mass $\hat{r}_1(v)$, plotted against those for wing area $\hat{r}_1(S)$; - (4) Radius of the gyration of the wing mass $\hat{r}_2(m)$, plotted against the position of the centre of mass $\hat{r}_1(m)$ [the curves show the allometric relationships for each species]; - (5) Radius of gyration \hat{l}_2 for the odonate body about the wing base, plotted against distance \hat{l}_1 from that axis to the centre of mass [the solid line shows the relationship obtained by least-squares linear regression].



- *Aeshna cyanea*
- *Libellula quadrimaculata*
- *L. depressa*
- × *Orthetrum cancellatum*
- ◇ *Sympetrum striolatum*
- ◆ *S. sanguineum*
- ▲ *Calopteryx splendens*

BODY PARAMETERS

The measured body parameters are given in Table III, and the relationship between \hat{l}_2 and \hat{l}_1 is shown in Figure 5.

The centre of mass occurred between the wing bases for all the percher anisopterans except *L. depressa*; this will maximise manoeuvrability by maximising the responsiveness of the body to turning torques from the wings. *L. depressa*, the broad-bodied chaser, is unusual in that its abdomen is relatively short and wide compared to the other perchers, and in the male this abdomen is a very conspicuous powder blue; this broad abdomen is probably used as a sexual signal for the male at the expense of a loss of manoeuvrability during flight. The centre of mass for the flier *A. cyanea* occurred behind the wing bases, confirming NEWMAN's (1982) distinction between the two behavioural groups. The damselfly *C. splendens*

Table III
Morphological body parameters

| species | sex | ID | L mm | m mg | m _b mg | m _m mg | m _m | \hat{l} | \hat{l}_1 | \hat{l}_2 | \hat{l}_b mg m ² |
|---------------------------------|-----|--------|---------|---------|----------------------|----------------------|----------------|-----------|-------------|-------------|----------------------------------|
| <i>Aeshna cyanea</i> | M | AC1 | 74.32 | 677.1 | 665.3 | | | 0.236 | 0.094 | 0.224 | 185.47 |
| | F | AC2 | 72.94 | 1085.6 | 1035.8 | 369.3 | 0.340 | 0.304 | 0.137 | 0.286 | 452.33 |
| | F | AC3 | 71.63 | 1162.3 | 1115.0 | 369.9 | 0.318 | 0.312 | 0.149 | 0.285 | 465.19 |
| | F | AC4 | 78.49 | 818.2 | 775.9 | 291.3 | 0.356 | 0.267 | 0.112 | 0.268 | 346.42 |
| | F | AC5 | 75.27 | 644.7 | 612.6 | 218.2 | 0.338 | 0.253 | 0.126 | 0.268 | 250.05 |
| | F | AC6 | | 567.6 | 539.5 | 196.2 | 0.346 | | | | |
| <i>Libellula depressa</i> | M | LD1 | 45.50 | 443.6 | 422.7 | | | 0.368 | 0.161 | 0.377 | 123.99 |
| | M | LD2 | 45.46 | 471.0 | | | | | | | |
| <i>Libellula quadrimaculata</i> | M | LQ16 | 46.99 | 373.8 | 353.3 | | | 0.301 | 0.079 | | |
| | M | LQ18 | 47.00 | 295.0 | 262.1 | | | 0.296 | 0.055 | | |
| | M | LQ29 | 47.31 | 385.0 | 361.6 | | | 0.295 | 0.078 | 0.257 | 53.80 |
| | M | LQ30 | 45.97 | 377.9 | 354.2 | 183.5 | 0.486 | 0.315 | 0.128 | 0.261 | 50.67 |
| | M | LQ31 | 46.76 | 408.9 | 385.5 | 186.6 | 0.456 | 0.324 | 0.129 | 0.265 | 58.99 |
| <i>Orbhetrum cancellatum</i> | M | OC1 | 46.83 | 415.8 | 394.1 | | | 0.294 | 0.082 | 0.216 | 40.18 |
| | M | OC2 | 48.43 | 449.1 | 426.9 | 243.8 | 0.543 | 0.306 | 0.122 | 0.257 | 66.18 |
| | M | OC3 | 48.28 | 443.7 | 419.3 | 233.3 | 0.526 | | | | |
| | M | OC4 | 49.31 | 443.1 | 421.8 | 227.1 | 0.513 | 0.320 | 0.122 | 0.258 | 65.27 |
| | M | OC5 | 47.32 | 415.0 | 387.6 | 210.9 | 0.508 | 0.291 | 0.115 | 0.243 | 50.97 |
| | M | OC6 | 46.39 | 382.1 | 362.0 | 199.2 | 0.521 | 0.279 | 0.093 | 0.232 | 42.38 |
| | M | OC7 | 49.48 | 350.7 | 332.8 | 179.4 | 0.512 | 0.279 | 0.055 | 0.184 | 27.60 |
| <i>Sympetrum sanguineum</i> | M | SSan1 | 34.15 | 135.3 | 127.4 | 65.5 | 0.484 | 0.256 | 0.056 | 0.192 | 5.46 |
| | M | SSan2 | 34.29 | 121.9 | 115.3 | 60.0 | 0.492 | 0.278 | 0.075 | 0.239 | 7.77 |
| | M | SSan3 | 34.81 | 114.0 | 109.1 | 56.1 | 0.492 | 0.273 | 0.073 | 0.200 | 5.34 |
| | M | SSan4 | 33.88 | 125.5 | 120.8 | 61.3 | 0.489 | 0.279 | 0.063 | 0.217 | 6.52 |
| | M | SSan5 | 33.64 | 133.0 | 125.9 | 64.3 | 0.483 | 0.280 | 0.041 | 0.173 | 4.34 |
| | M | SSan6 | 31.64 | 111.5 | 105.3 | 53.5 | 0.479 | 0.255 | 0.053 | 0.205 | 4.45 |
| | M | SSan7 | 34.40 | 138.5 | 131.3 | 69.9 | 0.505 | 0.270 | 0.078 | 0.253 | 9.92 |
| | M | SSan8 | 33.30 | 108.4 | 102.8 | 49.9 | 0.460 | 0.248 | 0.032 | 0.197 | 4.39 |
| | M | SSan9 | 36.72 | 139.3 | 131.6 | 68.1 | 0.489 | 0.270 | 0.074 | 0.259 | 11.86 |
| | M | SSan10 | 34.26 | 133.6 | 125.8 | 63.4 | 0.475 | 0.282 | 0.077 | 0.228 | 7.69 |
| <i>Sympetrum striolatum</i> | M | SS1 | 43.12 | 153.9 | 142.3 | | | 0.265 | 0.065 | 0.241 | 16.73 |
| | F | SS2 | 42.54 | 122.9 | 113.6 | | | 0.259 | 0.088 | 0.243 | 12.11 |
| | F | SS3 | 43.40 | 112.7 | 102.7 | | | 0.268 | 0.077 | 0.247 | 11.76 |
| | M | SS4 | 41.79 | 108.0 | 99.3 | | | 0.272 | 0.113 | 0.268 | 12.52 |
| | F | SS5 | 42.32 | 118.9 | 108.4 | | | 0.270 | 0.096 | 0.243 | 11.44 |
| | M | SS6 | 41.81 | 125.9 | 116.1 | | | 0.246 | 0.041 | 0.207 | 8.72 |
| | M | SS7 | 43.28 | 109.1 | 100.2 | | | 0.256 | 0.066 | 0.228 | 9.77 |
| | M | SS8 | 43.00 | 131.7 | 121.5 | | | 0.266 | 0.035 | 0.164 | 6.15 |
| <i>Calopteryx splendens</i> | M | CS1 | 45.28 | 91.0 | 81.9 | 29.7 | 0.327 | 0.264 | 0.089 | 0.279 | 13.14 |
| | M | CS2 | 43.37 | 93.6 | 85.9 | 34.3 | 0.367 | 0.311 | 0.126 | 0.330 | 17.60 |
| | M | CS3 | 47.16 | 123.6 | 113.4 | 42.3 | 0.342 | 0.315 | 0.146 | 0.342 | 29.42 |
| | M | CS4 | 48.36 | 119.1 | 108.8 | 42.0 | 0.353 | 0.324 | 0.165 | 0.339 | 29.27 |
| | M | CS5 | | 105.6 | 98.7 | 39.3 | 0.372 | | | | |
| | M | CS6 | 47.97 | 88.2 | 80.4 | 29.8 | 0.337 | 0.278 | 0.133 | 0.319 | 18.86 |
| | M | CS7 | 44.74 | 81.8 | 75.7 | 28.9 | 0.353 | 0.256 | 0.103 | 0.285 | 12.24 |

also had a centre of mass behind its wing bases, but this does not necessarily represent a loss of manoeuvrability because zygopterans can change direction by altering the position of their stroke planes without needing to change their body attitude (WAKELING & ELLINGTON, 1997b). The least-squares linear regression describing the relation of \hat{l}_2 with \hat{l}_1 is given by

$$\hat{l}_2 = 1.154 \hat{l}_1 + 0.142. \quad (20)$$

The non-dimensional muscle mass \hat{m}_m was less for the flier than for the percher anisopterans. MAY (1981) notes that this is due to both a lower thoracic mass and a smaller thoracic volume fraction of flight muscle in fliers.

DISCUSSION

In his study on the morphologies of the wings from six insect orders, ELLINGTON (1984a) noted that there were general laws of wing shape and that the radii of the moments of area and virtual mass could be predicted from $\hat{r}_1(S)$ using allometric relationships. The allometric relationships between the radii of wing mass and $\hat{r}_1(S)$ were not strong enough to be of predictive value, and so he suggested additionally determining the position of the centre of mass, $\hat{r}_1(m)$, by balancing the wing on a knife edge. Data for these radii for six butterfly species (BETTS & WOOTTON, 1988) showed allometries that were not significantly different from those in the ELLINGTON (1984a) analysis, thus reinforcing the idea of general laws of shape. Further studies on butterfly morphologies (DUDLEY, 1990; BUNKER, 1993) revealed shape and virtual mass allometries that were significantly different from Ellington's, although the radii of the moments of mass were not. Dudley attributed these differences to the fact that his analysis was of butterflies with wing areas much more skewed distally than for the insects previously studied. Dudley then states that "... while wing mass distributions may be conservative across the Insecta, wing area distributions are not necessarily so". The present study shows that the odonatan allometric relationships for the radii of area and virtual mass are significantly slightly different from the general relationships given by Ellington, but that the radii for the moments of mass are very variable and depend on the nature of the pterostigmas in the wings. Whereas the relationships derived from a broad range of insects (ELLINGTON, 1984a) are a good general starting point for predicting the radii of the moments of morphological parameters, it should be remembered that within a particular insect order the wing shapes may differ from the norm. Particular care should be exercised when using allometric relationships to predict wing parameters which may be affected by the peculiarities of particular insect groups, for example butterfly planforms or dragonfly mass distributions.

The moment parameters of the wings give a global description of their shape. There are times, however, when an analytical description of shape is required, for

example during a quasi-steady analysis of flight aerodynamics (WAKELING & ELLINGTON, 1997c). ELLINGTON (1984a) describes a Beta distribution that can be used to predict the normalised chord $\hat{c} = c/\bar{c}$ in terms of radial position \hat{r} . This distribution can be expressed by

$$\hat{c} = \hat{r}^{p-1}(1-\hat{r})^{q-1} \frac{\Gamma(p+q)}{\Gamma(p)\Gamma(q)}, \quad (21)$$

where $\Gamma()$ is a Euler gamma function, and the parameters p and q are the following functions of the moments of area,

$$p = \hat{r}_1(S) \left\{ \left[\frac{\hat{r}_1(S)(1-\hat{r}_1(S))}{\hat{r}_2^2(S)-\hat{r}_1^2(S)} \right] - 1 \right\}, \quad (22)$$

$$q = (1-\hat{r}_1(S)) \left\{ \left[\frac{\hat{r}_1(S)(1-\hat{r}_1(S))}{\hat{r}_2^2(S)-\hat{r}_1^2(S)} \right] - 1 \right\}. \quad (23)$$

The Beta distribution is compared with the measured values for \hat{c} in Figure 6 for both anisopteran and zygoptera fore- and hindwings; it can be seen that the distributions give remarkably good fits across the entire range of \hat{r} regardless of wing shape.

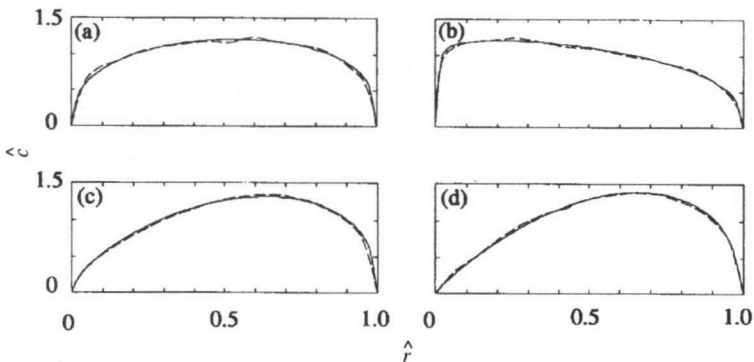


Fig. 6. Comparison between the non-dimensional chord (\hat{c}) measured along the wing length (\hat{r}) (dashed line) and the Beta distribution obtained by matching moments (solid line), for the four types of wing: (a) *Sympetrum sanguineum* forewing (SSan1); – (b) *S. sanguineum* hindwing (SSan1); – (c) *Calopteryx splendens* forewing (CS1); – (d) *C. splendens* hindwing (CS1). – [Abbreviations follow those in Tabs I-III.]

WING MORPHOLOGIES FOR ANISOPTERANS AND ZYGOPTERANS

The precise phylogeny of the Odonata is still under debate (for example FRASER, 1954; HENNIG, 1981; PFAU, 1991) and it is not the role of this study to enter into this discourse. It is generally accepted, however, that the Anisoptera are a monophyletic group which is derived from zygopteran lineage. The zygopteran wing form of identical fore- and hindwings, also seen in the Anisozygoptera, is the ancestral condition, and the Anisoptera have later developed modified wings that are no longer identical. Each wing form has its advantages, and these are outlined below.

The zygopteran wings, which stem from a narrow base and enlarge to concentrate their area in the outer half, show a good adaptation to the clap and fling wingbeats which the damselflies typically perform (RUDOLPH, 1976; MARDEN, 1987). The clap and fling mechanism is peculiar to zygopterans, and is the reason for the high aerodynamic performance that they achieve from their wings (WAKELING & ELLINGTON, 1997b, 1997c). To perform a perfect fling the wings begin with their surfaces touching and then fling open, leading edge first, until they finally come apart as the trailing edges separate. For insects with a small wing base separation, like the zygopterans, the wings need to taper into a narrow base if they are to maximise the contact time of the trailing edge during the fling; hence the petiole nature of their wing planform.

Anisopterans are generally larger than zygopterans, and their higher wing loading means that they typically fly faster. Frequent flights at higher speeds benefit from the wing area being more evenly distributed along the span than is the case for zygopterans. The reason for anisopteran forewings having a different planform to their hindwings can again be attributed to wingbase separation. The gap between the fore- and hindwing bases is relatively small, and the forewing is unable to have an enlarged wingbase without physically interfering with the hindwing; additional wing area cannot be placed ahead of the leading edge because this acts as a structural girder which could not support additional frontal area. The hindwing is able to increase its area near the base, and this has been done to a greater extent than in the forewing.

WING MORPHOLOGIES FOR FLIERS AND PERCHERS

To draw conclusions on differences between the wing morphologies for anisopteran fliers and perchers requires more information because only one flier species, *A. cyanea*, was caught during the study. CORBET (1983) states that members of the Aeshnidae and Corduliidae are typically fliers, and the Gomphidae and Libellulidae are typically perchers, and so values of $\hat{r}_1(S)$ for seven species from each of these families were compared to test whether fliers have different wing planforms from perchers. Where $\hat{r}_1(S)$ was not available from species caught in

this study, the wing planforms from ASKEW (1988) were used; he traced these from projected images to preserve correct shape and proportions. The results are shown in Table IV. The different families have characteristic wing planforms (as measured by $\hat{r}_1(S)$) but the planforms are not significantly different between fliers and perchers. The different flight behaviour of fliers and perchers has not led to the evolution of differently shaped wings for each group.

Table IV

Non-dimensional radii for the centroids of wing area for Anisoptera; data from this study and drawings in ASKEW (1988)

| Behaviour | Family | Species | Forewing $\hat{r}_1(S)$ | Hindwing $\hat{r}_1(S)$ |
|-----------|--------------|---------------------------------|-------------------------|-------------------------|
| FLIERS | Aeshnidae | <i>Aeshna juncea</i> | 0.51 | 0.48 |
| | | <i>A. cyanea</i> | 0.51 | 0.47 |
| | | <i>A. grandis</i> | 0.53 | 0.49 |
| | | <i>Anax imperator</i> | 0.50 | 0.48 |
| | | <i>A. parthenope</i> | 0.51 | 0.48 |
| | | <i>Brachytron pratense</i> | 0.52 | 0.49 |
| | | <i>Boyeria irene</i> | 0.53 | 0.48 |
| | Corduliidae | <i>Cordulia aenea</i> | 0.52 | 0.48 |
| | | <i>Somatochlora metallica</i> | 0.51 | 0.47 |
| | | <i>S. alpestris</i> | 0.50 | 0.47 |
| | | <i>S. flavomaculata</i> | 0.51 | 0.47 |
| | | <i>Epitheca bimaculata</i> | 0.49 | 0.44 |
| | | <i>Oxygastra curtisi</i> | 0.51 | 0.46 |
| | | <i>Macromia splendens</i> | 0.50 | 0.47 |
| | | <i>Macromia splendens</i> | 0.50 | 0.47 |
| PERCHERS | Libellulidae | <i>Libellula quadrimaculata</i> | 0.51 | 0.45 |
| | | <i>L. depressa</i> | 0.50 | 0.45 |
| | | <i>Orthetrum cancellatum</i> | 0.50 | 0.44 |
| | | <i>Sympetrum striolatum</i> | 0.51 | 0.45 |
| | | <i>S. sanguineum</i> | 0.51 | 0.45 |
| | | <i>Leucorrhinia dubia</i> | 0.52 | 0.47 |
| | | <i>L. rubicunda</i> | 0.51 | 0.45 |
| | Gomphidae | <i>Gomphus flavipes</i> | 0.52 | 0.48 |
| | | <i>G. vulgatissimus</i> | 0.52 | 0.49 |
| | | <i>G. pulchellus</i> | 0.53 | 0.49 |
| | | <i>G. graslini</i> | 0.52 | 0.49 |
| | | <i>Ophiogomphus cecilia</i> | 0.50 | 0.48 |
| | | <i>Onychogomphus forcipatus</i> | 0.52 | 0.48 |
| | | <i>O. uncatas</i> | 0.52 | 0.49 |
| | | <i>O. uncatas</i> | 0.52 | 0.49 |

REFERENCES

- ASKEW, R.R., 1988. *The dragonflies of Europe*. Harley Books, Colchester.
- BETTS, C.R. & R.J. WOOTTON, 1988. Wing shape and flight behaviour in butterflies (Lepidoptera: Papilionoidea and Hesperioidea): a preliminary analysis. *J. exp. Biol.* 138: 271-288.
- BRODSKY, A.K., 1994. *The evolution of insect flight*. Oxford Sci. Publs, Oxford.

- BUNKER, S.J., 1993. *Form, flight pattern and performance in butterflies (Lepidoptera: Papilionoidea and Hesperioidea)*. PhD. thesis, Univ. Exeter.
- CHAI, P. & R.B. SRYGLEY, 1990. Predation and the flight, morphology and temperature of neotropical rain-forest butterflies. *Am. Nat.* 135: 748-765.
- CORBET, P.S., 1983. *A biology of dragonflies*. Classey, Farrington, Oxon.
- D'ANDREA, M. & S. CARFI, 1988. Spines on the wing veins in Odonata. 1. Zygotera. *Odonatologica* 17: 313-335.
- D'ANDREA, M. & S. CARFI, 1989. Spines on the wing veins in Odonata. 2. Anisozygotera and Anisoptera. *Odonatologica* 18: 147-178.
- DUDLEY, R., 1990. Biomechanics of flight in neotropical butterflies: morphometrics and kinematics. *J. exp. Biol.* 150: 37-53.
- ELLINGTON, C.P., 1984a. The aerodynamics of hovering insect flight. 2. Morphological parameters. *Phil. Trans. R. Soc. Lond. (B)* 305: 17-40.
- ELLINGTON, C.P., 1984b. The aerodynamics of hovering insect flight. 6. Lift and power requirements. *Phil. Trans. R. Soc. Lond. (B)* 305: 145-181.
- ENNOS, A.R., 1988. The importance of torsion in the design of insect wings. *J. exp. Biol.* 140: 137-160.
- ENNOS, A.R., 1989. The effect of size on the optimal shapes of gliding insects and seeds. *J. Zool. Lond.* 219: 61-69.
- FRASER, F.C., 1954. The origin and descent of the order Odonata based on the evidence of persistent archaic characters. *Proc. R. ent. Soc. Lond. (B)* 23: 89-95.
- GRABOW, K. & G. RUPPELL, 1995. Wing loading in relation to size and flight characteristics of European Odonata. *Odonatologica* 24: 175-186.
- HENNIG, W., 1981. *Insect phylogeny*. Wiley, Chichester, New York.
- HERTEL, H., 1966. Membranous wing of insects. In: *Structure-form-movement*, pp. 78-87, Reinhold, New York.
- MAGNAN, A., 1934. *La locomotion chez les animaux. 1. Le vol des insectes*. Hermann, Paris.
- MARDEN, J.H., 1987. Maximum lift production during takeoff in flying animals. *J. exp. Biol.* 130: 235-258.
- MARDEN, J.H., 1989. Bodybuilding dragonflies: costs and benefits maximising flight muscle. *Physiol. Zool.* 62: 505-521.
- MAY, M.L., 1981. Allometric analysis of body and wing dimensions of male Anisoptera. *Odonatologica* 10: 279-291.
- NEVILLE, A.C., 1960. *The functions of the flight muscles, axillary sclerites and associated structures during the wingstroke cycle of Odonata*. PhD. thesis, Univ. London.
- NEWMAN, B.G., S.B. SAVAGE & D. SCHOUELLA, 1977. Model tests on a wing section of an *Aeschna* dragonfly. In: T.J. Pedley, [Ed.], *Scale effects in animal locomotion*, pp. 445-477, Acad. Press, London.
- NEWMAN, D.J.S., 1982. *The functional wing morphology of some Odonata*. PhD. thesis, Univ. Exeter.
- NEWMAN, D.J.S. & R.J. WOOTTON, 1986. An approach to the mechanics of pleating in dragonfly wings. *J. exp. Biol.* 125: 361-372.
- NORBERG, R.Å., 1972. The pterostigma of insect wings an inertial regulator of wing pitch. *J. comp. Physiol.* 81: 9-22.
- NORBERG, U.M. & J.M.V. RAYNER, 1987. Ecological morphology and flight in bats (Mammalia: Chiroptera): wing adaptations, flight performance, foraging strategy and echolocation. *Phil. Trans. R. Soc. (B)* 316: 335-427.
- PFAU, H.K., 1986. Untersuchungen zur Konstruktion, Funktion und Evolution des Flugapparates der Libellen. *Tijdschr. Ent.* 129: 35-123.
- PFAU, H.K., 1991. Contributions of functional morphology to the phylogenetic systematics of Odonata. *Adv. Odonatol.* 5: 109-141.

- PRANDTL., L. & O.G. TIETJENS, 1957. *Applied hydro- and aeromechanics*. Dover, New York.
- REES, C.J.C., 1975a. Form and function in corrugated insect wings. *Nature, Lond.* 256: 200-203.
- REES, C.J.C., 1975b. Aerodynamic properties of an insect wing section and a smooth aerofoil compared. *Nature, Lond.* 258: 141-142.
- RUDOLPH, R., 1976. Some aspects of wing kinematics in *Calopteryx splendens* (Harris) (Zygoptera: Calopterygidae). *Odonatologica* 5: 119-127.
- RUPPELL, G., 1989. Kinematic analysis of symmetrical flight manoeuvres of Odonata. *J. exp. Biol.* 144: 13-42.
- RÜPPELL, G., & D. HILFERT, 1993. The flight of the relict dragonfly *Epiophlebia superstes* in comparison with that of the modern Odonata (Anisozygoptera: Epiophlebiidae). *Odonatologica* 22: 295-309.
- SCHLICHTLING, H., 1968. *Boundary-Layer Theory*. [6th edn] McGraw-Hill, New York.
- SRYGLEY, R.B. & R. DUDLEY, 1993. Correlations of the position of center of body mass with butterfly escape tactics. *J. exp. Biol.* 174: 155-166.
- WAKELING, J.M. & C.P. ELLINGTON, 1997a. Dragonfly flight. 1. Gliding flight and steady-state aerodynamics. *J. exp. Biol.* [In press]
- WAKELING, J.M. & C.P. ELLINGTON, 1997b. Dragonfly flight. 2. Velocities, accelerations and kinematics of flapping flight. *J. exp. Biol.* [In press]
- WAKELING, J.M. & C.P. ELLINGTON, 1997c. Dragonfly flight. 3. Lift and power requirements. *J. exp. Biol.* [In press]
- WEIS-FOGH, T., 1973. Quick estimates of flight fitness in hovering animals, including novel mechanisms for lift production. *J. exp. Biol.* 59: 169-230.
- WOOTTON, R.J., 1991. The functional morphology of the wings of Odonata. *Adv. Odonatol.* 5: 153-169.